Egyptian Journal of Basic and Applied Sciences 5 (2018) 41–53

HOSTED BY

Contents lists available at ScienceDirect

Egyptian Journal of Basic and Applied Sciences

journal homepage: www.elsevier.com/locate/ejbas

Full Length Article

Molecular docking and QSAR analysis of a few Gama amino butyric acid aminotransferase inhibitors

Usman Abdulfatai *, Adamu Uzairu, Sani Uba

Department of Chemistry, Ahmadu Bello University, Zaria, Nigeria

ARTICLE INFO

Article history:
Received 23 June 2017
Received in revised form 5 January 2018
Accepted 8 January 2018
Available online 18 January 2018

Keywords:
QSAR
Gamma-aminobutyric acid aminotransferase
Molecular docking
Density Functional Theory
Anticonvulsants
Genetic Function Algorithm

ABSTRACT

Molecular docking and quantitative structure–activity relationship (QSAR) studies were carried out on 37 anticonvulsant compounds to develop a robust model for the prediction of anticonvulsant activities against Gama amino butyric acid aminotransferase ($GABA_{AT}$) and to determine the dominant structural amino acid residues responsible for the binding affinity of the ligand-$GABA_{AT}$ complex. AutoDock Vina of PyRx virtual screening software was used to perform the molecular docking while Genetic function algorithm (GFA) was used to select the descriptors and to generate the correlation models that relate the structural features to the biological activities. The best binding affinity was found to be −11.9 Kcal/mol (compound 5a) while best QSAR model (model 1) was obtained with R^2 of 0.970192, an R^2_{adj} value of 0.963095, Q^2LOO value of 0.947995 and R^2pred of 0.813. These confirms the stability, reliability, robustness and predictability of the model. Our research has shown that the binding affinity generated was found to be better than the one reported by another researcher. And the high correlation coefficient, (R^2) shows that the model was reliable, robust and predictable. Our QSAR model and molecular docking results corroborate with each other (most especially in the area of binding affinity and atomic electronegativity of the inhibitors) and propose the directions for the design of new inhibitors with better activity against an enzyme that is responsible for epilepsy (GABAAT).

1. Introduction

Epilepsy is a well-documented neurological issue that influences roughly 65 to 75 million individuals around the world, of which 10.5 million are children [1,2]. However, the worldwide prevalence of epilepsy varies from 2.8 to 19.5 per 1000 of the general population [3]. Epilepsy is basically a chronic brain disorder characterized by recurrent derangement of the nervous system due to the sudden excessive disorderly discharge of neurons that result in almost instantaneous disturbance of sensation and loss of consciousness [4]. Seizures which is usually caused by epilepsy can cause a variety of symptoms depending on the areas of the brain affected. Symptoms may be the complete or partial loss of consciousness, loss of speech and uncontrollable motor behavior [5].

The in silico approaches like Quantitative Gama amino butyric acid aminotransferase ($GABA_{AT}$) catalyzes the conversion of GABA to succinylic semialdehyde. Convulsion is always triggered by reduced levels of GABA, while the high level of GABA in the brain has an anticonvulsant effect [6–9]. $GABA_{AT}$ is a receptor for most anti-epileptic drugs because of its selective deactivation raises GABA concentration in the brain [10]. This understanding of GABA neurotransmitter paved the way for future research and some of the disorder's first effective treatments [11–13].

Structure-Activity Relationships (QSAR) and molecular docking are widely used in the fields of structural molecular biology and structure-based drug design. Molecular docking is a computational procedure used in the field of structure-based rational drug design to identify correct conformations of small molecule and also to estimate the strength of the protein-ligand interaction [14–16]. Quantitative Structure-Activity Relationships (QSAR) models have gained an extensive recognition in the field of sciences [17–24].

The aim of this research is to develop good and rational QSAR models that could predict the activities (pED_{50}) values of quinoxaline and thiadiazoles derivatives (inhibitors) whose biological activities (ED_{50}) against Gama amino butyric acid aminotransferase ($GABA_{AT}$) and to predict the interactions energy between $GABA_{AT}$ and the inhibitors

* Corresponding author at: Department of Chemistry, Ahmadu Bello University, P. M.B. 1044, Zaria, Nigeria.
E-mail address: faithyikare4me@gmail.com (U. Abdulfatai).

https://doi.org/10.1016/j.ejbas.2018.01.003
2314-808X/

2. Material and methods

2.1. Data sets used

Some quinoxaline and thiadiazoles derivatives were selected from the literature and used as anticonvulsant activity for this study [25–27]. The logarithm of measured ED_{50} against an anticonvulsant activity as pED_{50} ($pED_{50} = \log 1/ED_{50}$) was used as dependent variable, consequently correlating the data linearly to the independent variable/descriptors. The observed structures and the biological activities of these compounds are presented in Table 1.

2.2. Docking study

2.2.1. Selection and refinement of receptors

Computer-aided drug design involves the identification and selection of the appropriate drug target [28]. Gama amino butyric acid aminotransferase ($GABA_{AT}$) was the target for the quinoxaline and thiadiazoles derivatives, and the three-dimensional structure of this protein was retrieved from Protein Data Bank (www.rcsb.org/pdb) using PDB ID: 10HV. The target protein was prepared by removing water molecules, adding Polar hydrogen atoms, minimizing energy, and the structure was saved as the pdbqt format. Fig. 1 shows the prepared receptor ($GABA_{AT}$).

2.2.2. Ligand input file preparation and optimization

37 quinoxaline and thiadiazoles derivatives input structures were drawn using the graphic user interface of Spartan'14 version 1.1.2 software [29]. The drawn structures were cleaned in 3D format and optimized using Spartan'14 version 1.1.2 [29]. The resulting structures were then saved in pdb format for molecular docking studies.

2.2.3. Docking

The docking of the quinoxaline and thiadiazoles derivatives into the active site of $GABA_{AT}$ protein was carried out using AutoDock Vina of PyRx virtual screening software [30]. Autodock vina has been reported to be an effective tool capable of quickly and accurately predicting bound conformations and binding energies of ligands with macromolecular targets [31]. In the graphic user interface of PyRx virtual screening software, the grid box with a dimension of $60 \times 60 \times 60$ points and 0.375 Å grid spacing was used to cover the entire protein binding site and accommodate ligand to move freely. After docking searches were completed, the best conformation was chosen from the most populated cluster with the minimum binding energy (highest binding score). The interaction of docked protein-ligand complex conformations, including hydrogen bond and hydrophobic interactions were analyzed using Discovery Studio Visualizer 4.1, Ligplot and PyMol visualization software [32].

2.2.4. Geometry optimization and calculation of physiochemical properties

The Spartan'14 version 1.1.2 software [29] running on Toshiba Satellite, Dual-core processor window eight (8) operating system was used to draw the molecular structures of the quinoxaline and thiadiazoles derivatives. All the structures of these compounds were geometrically optimized by minimizing energy (see Fig. 2). The physicochemical properties of all the 37 compounds were calculated by means of Density functional theory (DFT) using the B3LYP methods and 6-31G* basis set. The lowest energy structure was used for each molecule to calculate their physicochemical properties. The optimized structures from the Spartan'14 version 1.1.2 [29] Quantum chemistry package were saved in SDF format and transferred to PaDEL-Descriptor version 2.18 toolkit [33] where the calculation of all the dimensional descriptors took place.

The 37 data sets descriptors generated from the PaDEL version 2.18 toolkit [33] were divided into training and test sets (see Fig. 2). The training sets were used to develop the model, while the test sets were used to test for the quality assurance of the model. The Material studio software version 8 was used to perform the correlation analysis between activity values of the molecules against GABAAT and the calculated descriptors. The Genetic Function Approximation (GFA) method in material studio software versions 8 was used to perform the regression analysis of the generated descriptors.

2.2.4. Quality assurance of the developed model

The reliability and predictive ability of the generated models were assessed by internal and external validation parameters. These validation parameters were compared with the minimum recommended value for the QSAR model standard [34] showed in Table 2.

2.2.5. Determination of descriptors variance inflation factor (VIF)

The best regression model was generated by considering all the possible combination of descriptors. Variance inflation factor (VIF) [35] was used to identifying the multi-collinearity among variables. The VIF for the regression coefficient is expressed as:

$$\mathrm{VIF} = \frac{1}{1 - R_i}$$

R_i represents the coefficient produced by regressing the descriptor xi against the other descriptors, X_i ($j \neq i$) If VIF was greater than 10, it was not considered as a model

2.2.6. Calculation of physiochemical descriptors

Physicochemical descriptors are an expression of quantitative structure of a molecule, which are lipophilic, electronic and steric in nature. Physicochemical descriptors used in this study are presented in Table 3.

3. Results and discussion

All the four developed QSAR models (1, 2, 3, and 4) were reported out of which model 1 was chosen as the best model for predicting the pED_{50} of anticonvulsant molecules due to its statistical significance. As shown in Table 2, the internal and external validation parameters of the model 1 conformed to the minimum standard for a stable, reliable, predictable and robust QSAR model. Furthermore, model 1 was chosen as the best model because the highest squared correlation coefficient (R^2) of 0.970, adjusted squared correlation coefficient (R^2_{adj}) value of 0.963, Leave one out (LOO) cross-validation coefficient (Q^2) value of 0.948 and the external validation (R^2_{ext}) of 0.813 were confirmed with the minimum recommended value (Table 2) for a generally acceptable QSAR model [34].

Model 1

$$\begin{aligned} pED_{50} &= 0.263140426 * \mathrm{minHBint4} + 0.457064694 * \mathrm{ETA\_Alpha} \\ &\quad - 0.000783610 * \mathrm{DPSA\text{-}1} - 0.122305663 * \mathrm{GRAV\text{-}5} \\ &\quad - 0.031052119 * \mathrm{WT.eneg} + 5.798523557.\ \mathrm{N} \\ &= 27, R^2_{pred} = 0.813043, R^2 = 0.970192, R^2_a = 0.963095, Q^2_{cv} \\ &= 0.947995. \end{aligned}$$

Table 1
Biological activities of training and test set derivatives.

S/N	Compound	pED_{50}	PRED.	Res.
1b	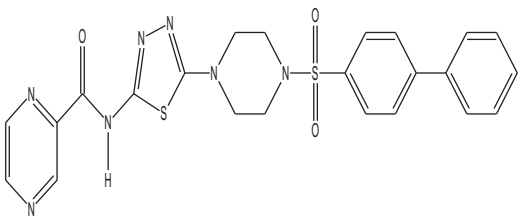	0.81	0.84	−0.03
2a	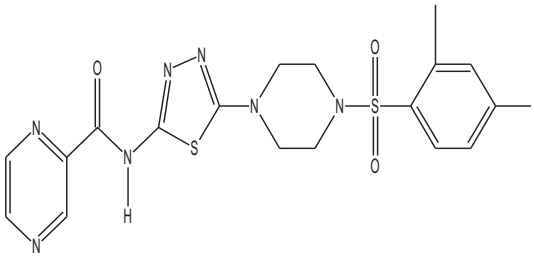	0.87	0.81	0.06
3a	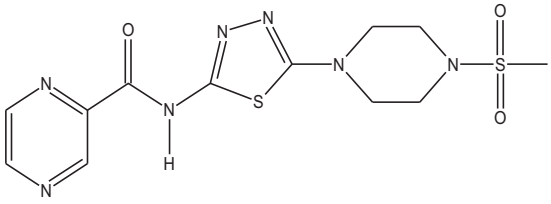	0.91	0.87	0.04
4a	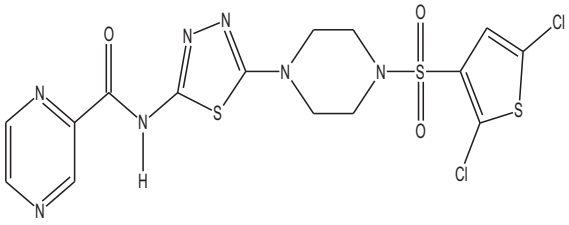	0.3	0.30	0
5a	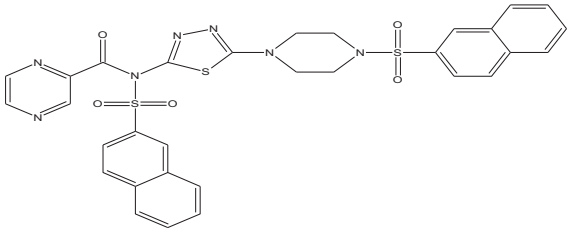	0.83	0.88	−0.05
6b	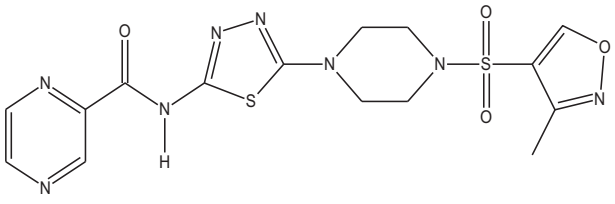	0.54	0.70	−0.16
7a	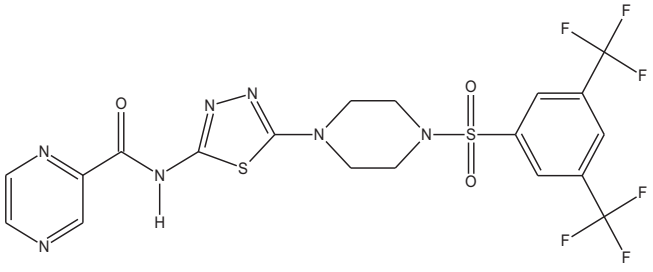	0.24	0.20	0.04

(*continued on next page*)

Table 1 (*continued*)

S/N	Compound	pED_{50}	PRED.	Res.
8a	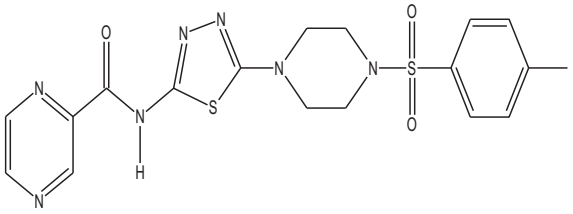	0.90	0.86	0.04
9a	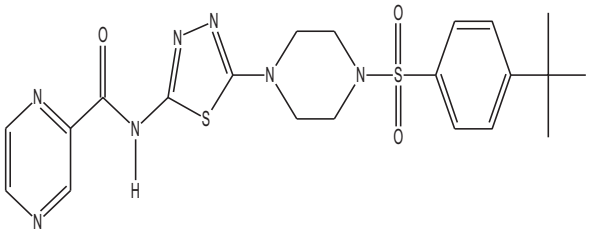	0.90	0.98	−0.08
10a	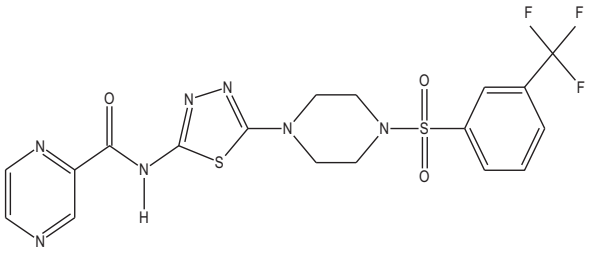	0.4	0.41	−0.01
11a	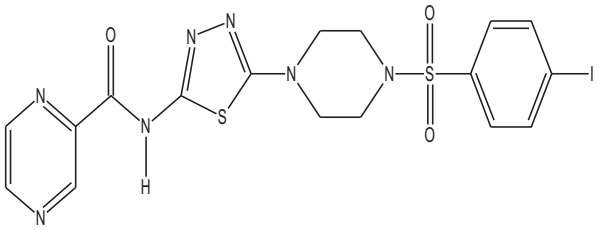	0.67	0.67	0
12a	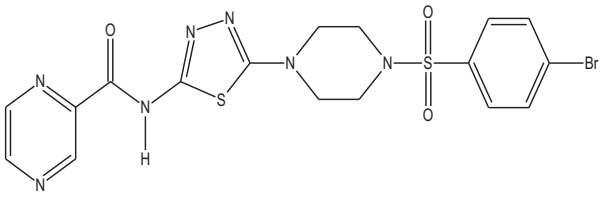	0.91	0.78	0.13
13b	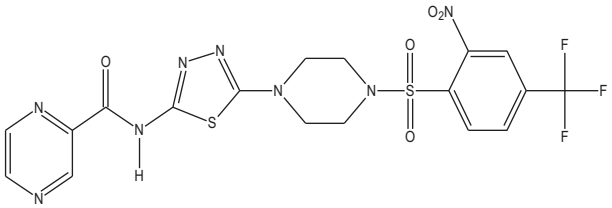	0.32	0.20	0.12
14a	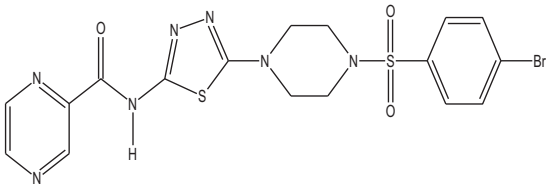	0.65	0.78	−0.13

Table 1 (*continued*)

S/N	Compound	pED_{50}	PRED.	Res.
15b	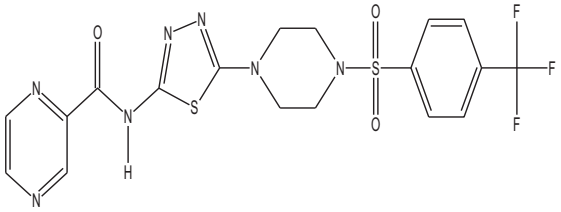	0.47	0.54	−0.07
16a	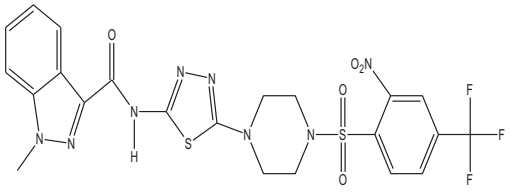	0.33	0.36	−0.03
17a	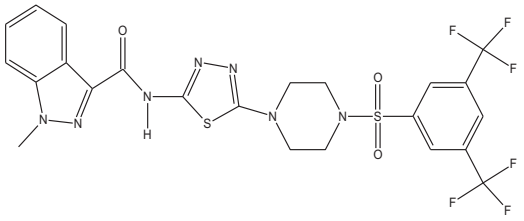	0.25	0.31	−0.06
18a	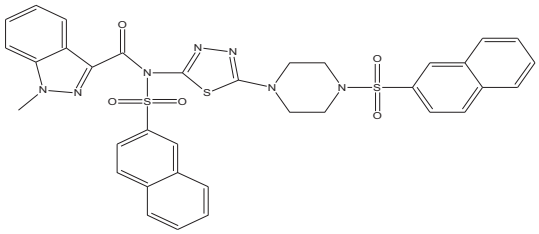	0.81	0.70	0.11
19a	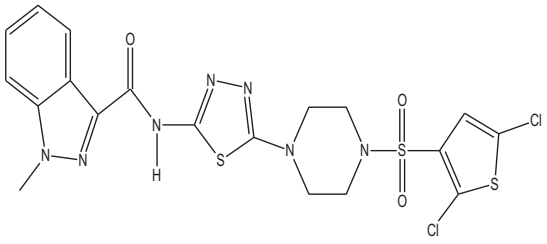	0.32	0.38	−0.06
20b	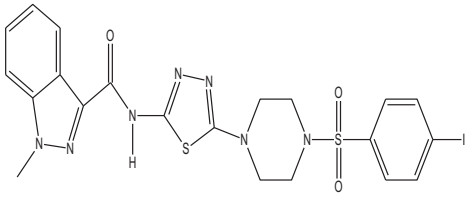	0.80	0.75	0.05
21a	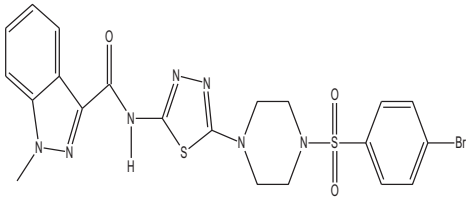	0.79	0.89	−0.1
22a	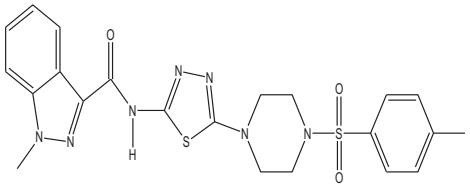	0.84	0.88	−0.04

(*continued on next page*)

Table 1 (*continued*)

S/N	Compound	pED_{50}	PRED.	Res.
23b	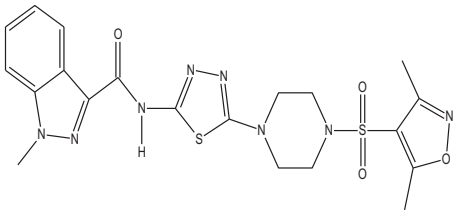	0.34	0.73	−0.39
24a	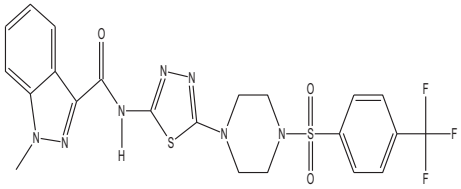	0.47	0.62	−0.15
25a	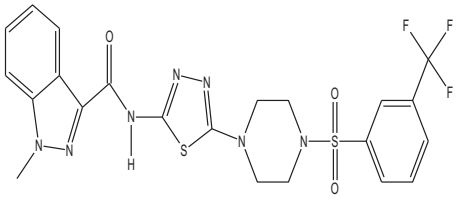	0.81	0.58	0.23
26b	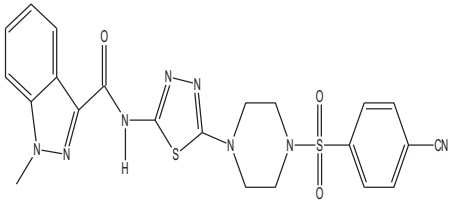	0.74	1.00	−0.26
27a	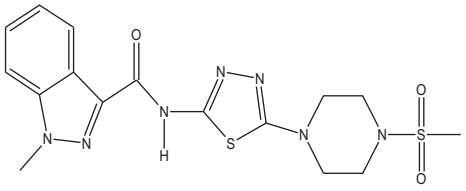	0.91	0.83	0.08
28a	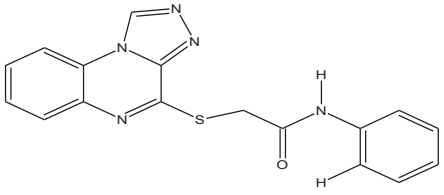	1.6	1.63	−0.03
29a	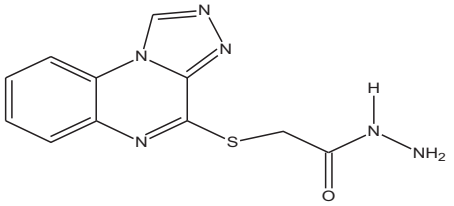	1.9	1.95	−0.5
30b	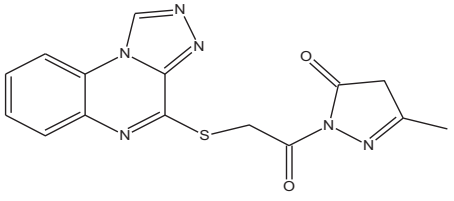	1.6	1.3	0.3

Table 1 (*continued*)

S/N	Compound	pED_{50}	PRED.	Res.
31a	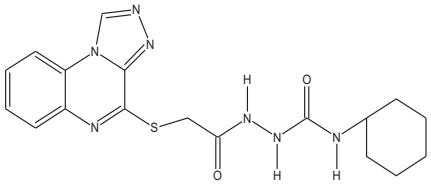	1.5	1.52	−0.02
32a	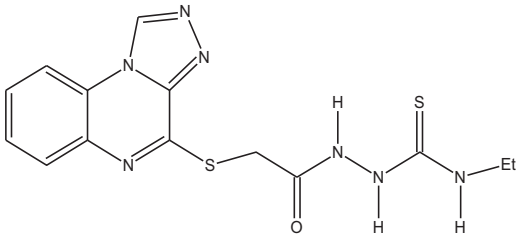	1.5	1.44	0.06
33a	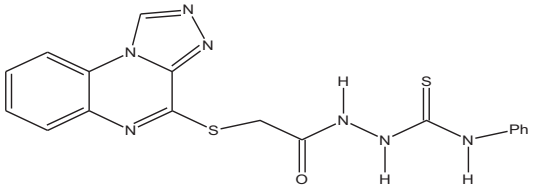	1.5	1.51	−0.01
34b	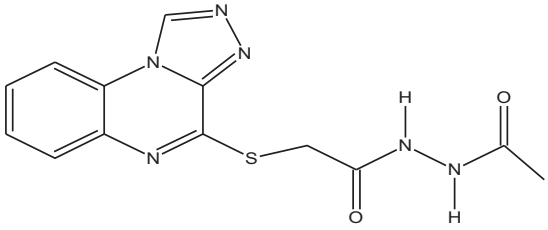	1.5	1.7	−0.2
35a	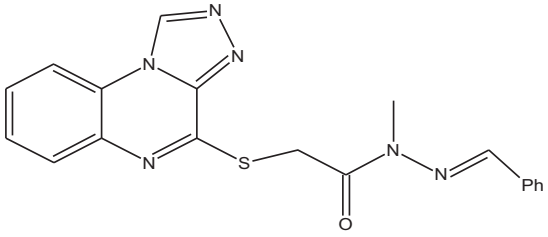	1.6	1.67	−0.07
36b	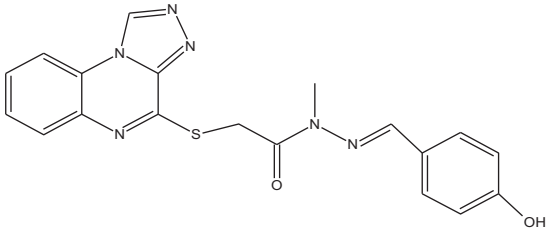	1.6	1.6	0
37a	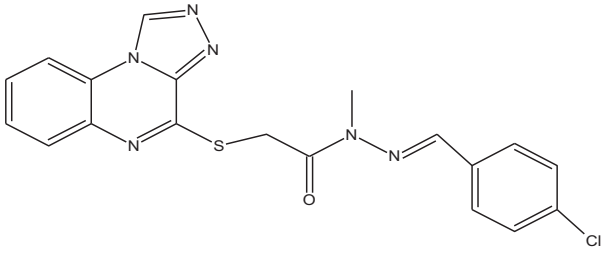	1.9	1.76	0.14

[a]Training set.
[b]Test set.

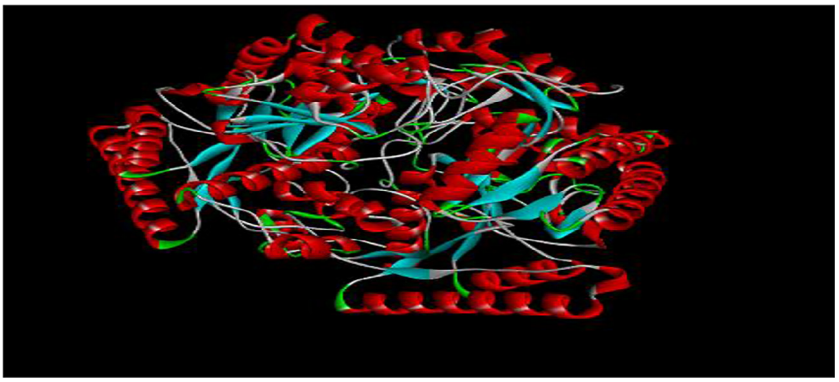

Fig. 1. Schematic diagram of receptor ($GABA_{AT}$).

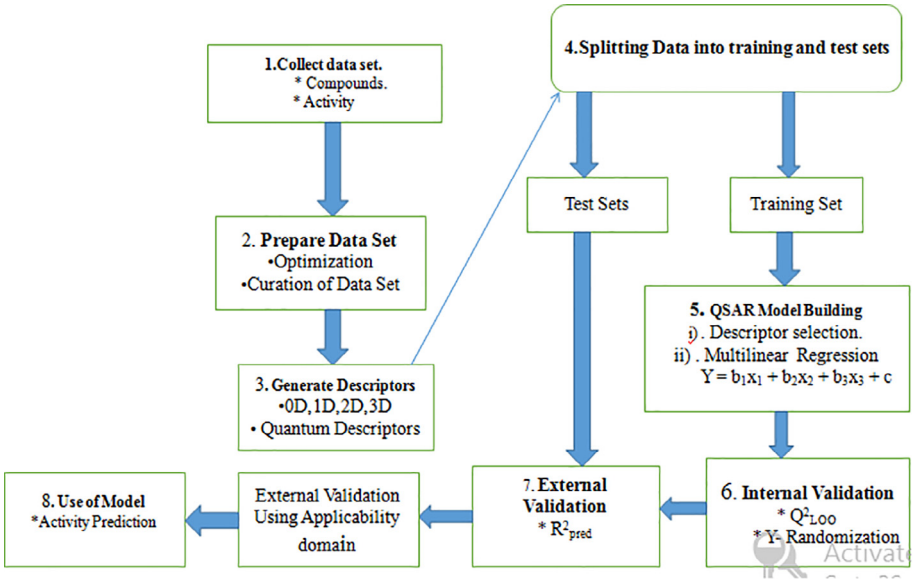

Fig. 2. QSAR procedure used in this work.

Table 2
Minimum recommended value of Validation Parameters for a generally acceptable QSAR model.

Name and Symbol	Value
Coefficient of determination R^2	≥0.6
Confidence interval at 95% confidence level $P_{(95\%)}$	<0.05
Cross validation coefficient Q^2	≥0.5
Difference between R^2 and Q^2 $R^2 - Q^2$	≤0.3
Minimum number of external test set $Next_{\text{test set}}$	≥5
Coefficient of determination for external test set R^2_{ext}	≥0.6

Model 2

$$pED50 = -0.263140426 * minHBint4 + 0.457064694 * RNCG - 0.000783610 * DPSA\text{-}1 - 0.122305663 * WD.unity - 0.031052119 * WK.unity + 5.798524.\ N = 27, R^2_{pred} = 0.812042, R^2 = 0.970112, R^2_a = 0.964095, Q^2_{cv} = 0.945995.$$

Model 3

$$pED50 = -0.264710141 * nHBint5 + 0.445962003 * VCH\text{-}7 + 0.445962003 * ETA\_Alpha - 1.310182695 * FPSA\text{-}1 - 0.120300596 * SCH\text{-}3 - 0.030766024 * nAtom + 6.440982.\ N = 27, R^2_{pred} = 0.811022, R^2 = 0.960112, R^2_a = 0.963095, Q^2_{cv} = 0.935995.$$

Model 4

$$pED50 = +0.263140426 * minaaNH - 0.557064694 * SaaCH - 0.000283610 * DPSA\text{-}1 + 0.222305663 * SHBint4 - 0.371052119 * WT.eneg + 7.799526.\ N = 27, R^2_{pred} = 0.811012, R^2 = 0.960012, R^2_a = 0.963094, Q^2_{cv} = 0.935993.$$

3.1. Plot of experimental versus predicted ED_{50} of both training and test sets of model 1

Fig. 3 gives the plot of predicted activities of both training and test sets against observed activities; the reliability of the model

Table 3
List of physicochemical descriptors selected for this study.

Full name	Description	Class
minHBint4	Minimum E-State descriptors of strength for potential Hydrogen Bonds of path length 4	2D
ETA_Alpha	Sum of alpha values of all non-hydrogen vertices of a molecule	2D
DPSA-1	Difference of PPSA-1 and PNSA-1	3D
GRAV-5	Square root of gravitational index of all pairs of atoms (not just bonded pairs)	3D
WT.eneg	Non-directional WHIM, weighted by Mulliken atomic electronegativites	3D

(best QSAR model) was confirmed as the GFA derived R^2 value was in agreement with the R^2 value of 0.970 recorded in this graph. The high Linearity of this plot indicates the high predictive power of the model.

3.2. Comparison of observed and predicted pED_{50} of model 1

The comparison of the predicted pED_{50} of the model 1 with its experimental values is presented in Table 4. The low residual values shown in the Table 4 confirm the high predictive power of the model

Table 4
Comparison of Observed, Predicted and Residual of Model 1.

Training Set No.	Observed pED_{50}	Pred. ED_{50}	Residual
2a	0.87	0.809319	0.060681
3a	0.91	0.879222	0.030778
4a	0.3	0.299784	0.000216
5a	0.83	0.879553	−0.04955
7a	0.24	0.200767	0.039233
8a	0.9	0.857363	0.042637
9a	0.9	0.98251	−0.08251
10a	0.4	0.410375	−0.01038
11a	0.67	0.668481	0.001519
12a	0.91	0.783826	0.126174
14a	0.65	0.783826	−0.13383
16a	0.33	0.359761	−0.02976
17a	0.25	0.314954	−0.06495
18a	0.81	0.703812	0.106188
19a	0.32	0.387612	−0.06761
21a	0.79	0.887411	−0.09741
22a	0.84	0.882509	−0.04251
24a	0.47	0.619185	−0.14919
25a	0.81	0.580288	0.229712
27a	0.91	0.832435	0.077565
28a	1.6	1.631665	−0.03166
29a	1.9	1.949181	−0.04918
31a	1.5	1.517619	−0.01762
32a	1.5	1.443062	0.056938
33a	1.5	1.515024	−0.01502
35a	1.6	1.666161	−0.06616
37a	1.9	1.764295	0.135705

3.3. External validation of model

Test set compounds of external validation of model 1 revealed a good agreement between the actual and predicted pED_{50} of the test set molecules. The actual, predicted and residual pED_{50} values of the test set compounds are presented in the Tables 5.

3.4. Calculation of predictive R^2 of model

The stability, reliability and robustness of the generated model 1 were confirmed by predictive R^2 (Tables 6). The calculated predictive R^2 for model 1 were in conformity with the standard value shown in Table 6.

3.5. Variance inflation factor (VIF) Statistic for the descriptors in model 1

The corresponding VIF values of the five descriptors are presented in Table 7. As can be seen from this table, all the variables has VIF values of less than 10, indicating that the obtained model

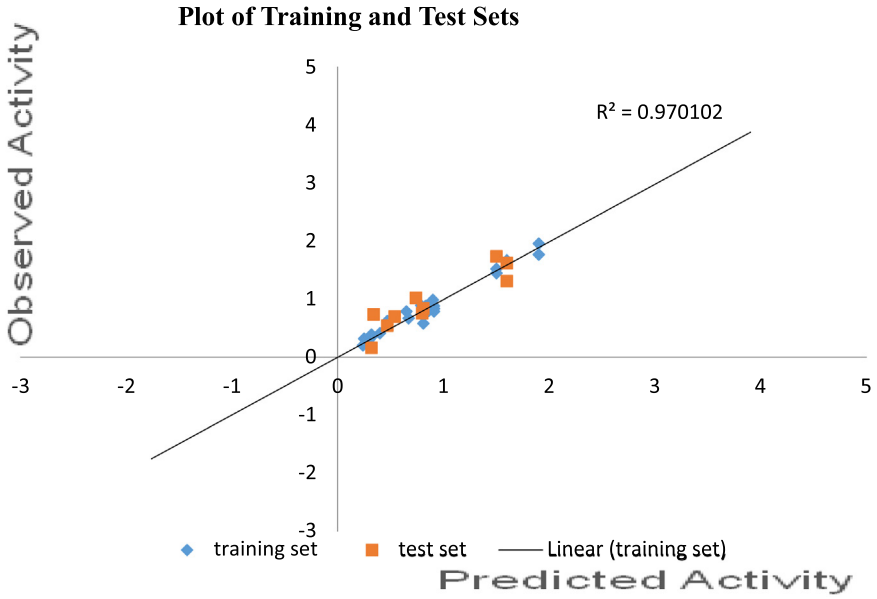

Fig. 3. Plot of training and test sets of model 1.

Table 5
External validation of Model 1.

Test Set No.	Exp. pED_{50}	minHBin4	ETA_Alpha	FPSA-1	GRAV-5	WT.eneg	Pred. pED_{50}	Residual
1b	0.81	1.094026	16.96665	0.6018	88.273	47.667	0.8435	−0.033
6b	0.54	1.100447	13.69998	0.5356	84.757	21.569	0.6976	−0.157
13b	0.32	1.00694	16.39044	0.46795	98.970	25.911	0.1674	0.1525
15b	0.47	1.052864	15.32378	0.4624	92.704	22.378	0.54932	−0.079
20b	0.8	0.806549	17.60951	0.5340	97.952	27.627	0.7472	0.0527
23b	0.34	0.811353	16.19998	0.5876	92.442	26.7940	0.7356	−0.3956
26b	0.74	0.807437	16.86665	0.5651	92.415	28.489	1.0144	−0.274
30b	1.6	0	11.39999	0.59454	73.634	19.185	1.2974	0.3026
34b	1.5	−1.04419	10.39999	0.5686	67.986	22.873	1.7277	−0.2277
36b	1.6	0	13.39999	0.57751	75.5558	31.0834	1.61448	−0.014

has statistical significance, and the descriptors were found to be reasonably orthogonal [35].

3.6. Result of molecular docking studies of quinoxaline and thiadiazoles derivatives

Molecular docking studies were carried out between the targets ($GABA_{AT}$) and its inhibitors (quinoxaline and thiadiazoles derivatives). In Table 7, all the compounds were found to strongly inhibit by completely occupying the active sites in the target protein ($GABA_{AT}$). All the $GABA_{AT}$ inhibitors showed lower energy values (higher docking scores) than the binding energies of vigabatrin (−4.4 kcal/mol), the standard antiepileptic drug. For target protein, binding energy values range from −5.8 to −11.9 kcal/mol. Furthermore, Fig. 4 shows the best first-three docking results

The positive coefficient in model 1 implies that increase in physiochemical parameters such as minHBint4 (Minimum E-State descriptors of strength for potential Hydrogen Bonds of path length 4), ETA_Alpha (Sum of alpha values of all non-hydrogen vertices of a molecule) and GRAV-5 (Square root of gravitational index of all pairs of atoms) will increases the anticonvulsant activities (pED_{50}) of these quinoxaline and thiadiazoles derivatives against $GABA_{AT}$ enzyme, an enzyme responsible for epilepsy. More also, negative coefficient of DPSA-1 (Difference of PPSA-1 and PNSA-1) and WT.eneg (Non-directional WHIM, weighted by Mulliken atomic electronegativity) are inversely proportional to the inhibitory activities of quinoxaline and thiadiazoles derivatives.

MinHBint4 (Minimum E-State descriptors of strength for potential Hydrogen Bonds of path length 4) is an electrotopological state atom type descriptor. In model 1, positive coefficient of this descriptor implies that increase in this descriptor will directly increase the inhibitory activities of the inhibitors against $GABA_{AT}$ enzyme, an enzyme that causes epilepsy. Furthermore, ETA_Alpha (Sum of alpha values of all non-hydrogen vertices of a molecule) and GRAV-5 (Square root of the gravitational index of all pairs of atoms) are extended topochemical atom and the gravitational index descriptors. These two descriptors (model 1) are directly proportional to the inhibitory activities (pED_{50}) of the quinoxaline and thiadiazoles derivatives (inhibitors). Therefore, increase the value of ETA_Alpha and GRAV-5 will lead to an increase in the inhibitory activities of quinoxaline and thiadiazoles derivatives against $GABA_{AT}$ enzyme.

Table 7
Variance Inflation Factor (VIF) Statistic for the Descriptors in Model 1.

S/NO	Dependent Variable	VIF
1	minHBint4	2.094696
2	ETA_Alpha	1.6935
3	DPSA-1	1.942884
4	GRAV-5	1.63697
5	WT.eneg	1.001944

DPSA-1 (Difference of PPSA-1 and PNSA-1), the charged partial surface area descriptor (CPSA) provides information that describes global and local electrophilicity in case of non-covalent molecular interactions [36]. Moreover, DPSA-1 descriptor provides separation information about high binding affinity to estrogen receptor [37]. Therefore, reduced level of DPSA-1 descriptor will increase the inhibitory activities of quinoxaline and thiadiazoles derivatives against an enzyme that causes epilepsy ($GABA_{AT}$).

WT.eneg (Non-directional WHIM, weighted by Mulliken atomic electronegativites) which is 3D, is defined as WHIM descriptor [38]. It encodes information about the weight of atomic electronegativites of the molecules ($GABA_{AT}$ inhibitors). The QSAR model (Model 1) pointed out that the pED_{50} (activities) of the inhibitors (quinoxaline and thiadiazoles derivatives) increases with the decrease in this descriptor. A critical look at this descriptor inferred that the atomic electronegativity in a molecule have to be reduced in order for the inhibitory activities of quinoxaline and thiadiazoles

Table 6
Calculation of Predictive R^2 of Model 4.10.

CP/NO	Y(te)	Ypred(te)	[Ypred(te)−Y(te)]2	Ym(tr)	[Y(te)−Ym(tr)]2
1	0.81	0.843524	0.001124	0.91	0.01
6	0.54	0.69762	0.024844	0.91	0.1369
13	0.32	0.167425	0.023279	0.91	0.3481
15	0.47	0.54932	0.006292	0.91	0.1936
20	0.8	0.747247	0.002783	0.91	0.0121
23	0.34	0.735629	0.156522	0.91	0.3249
26	0.74	1.014486	0.075342	0.91	0.0289
30	1.6	1.2974	0.091567	0.91	0.4761
34	1.5	1.727763	0.051876	0.91	0.3481
36	1.6	1.614488	0.00021	0.91	0.4761
			$\sum$ = 0.043		$\sum$ = 0.23

Therefore, Pred.R^2 = 1 − (0.043/0.23) = 0.813043.

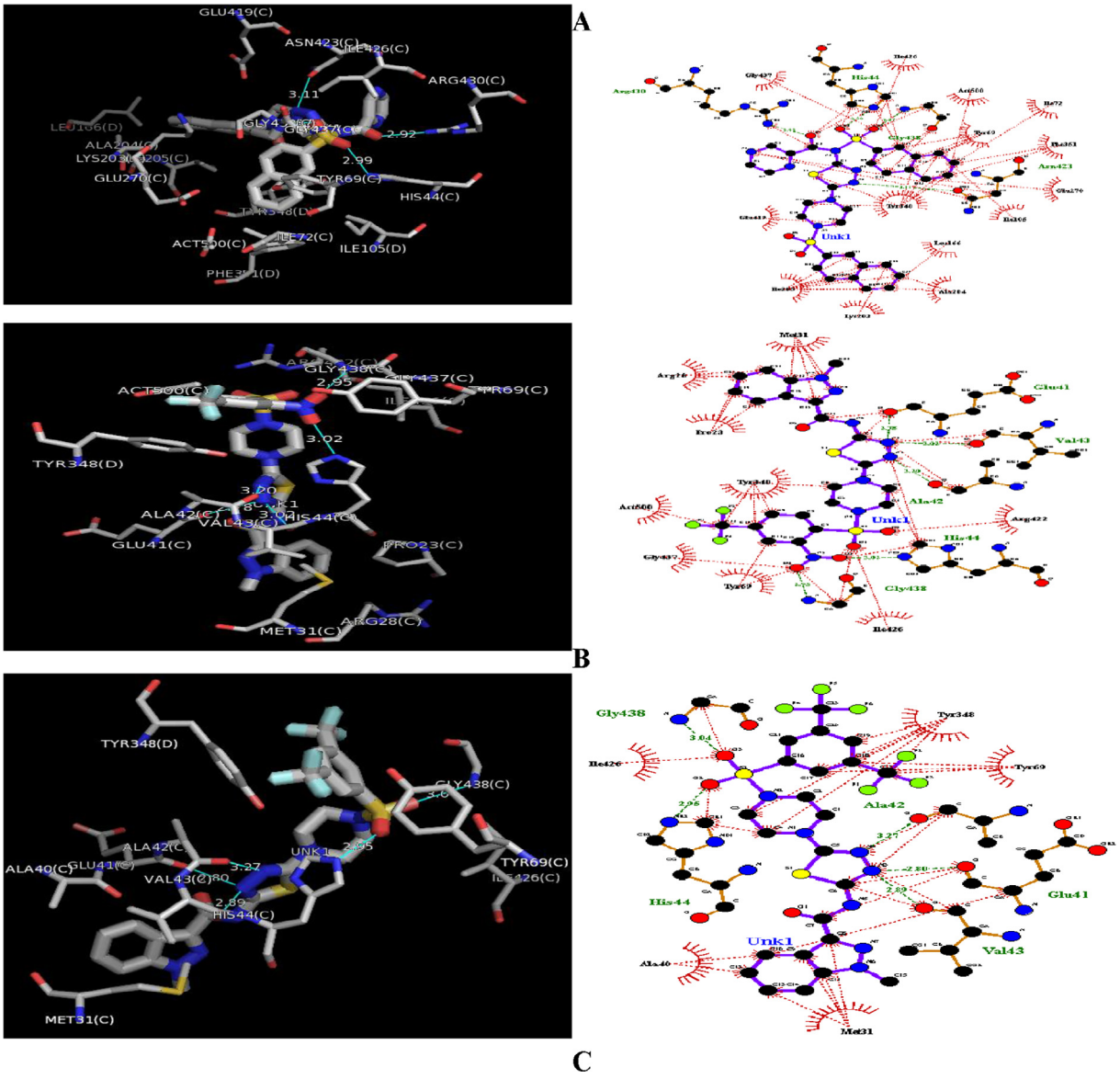

Fig. 4. 3D and 2D of (A): $GABA_{AT}$-Ligand 5a Complex. (B): $GABA_{AT}$-Ligand 16a Complex. (C): $GABA_{AT}$-Ligand 17a Complex. Ligand: H-bond interactions represented by green dashed lines: Hydrophobic interactions represented by red dashed line.

derivatives to be effective in inhibiting the activities of $GABA_{AT}$ enzyme, an enzyme responsible for epilepsy.

From the docking study, it was shown that quinoxaline and thiadiazoles ring of ligand number 5a (Table 8) with the highest binding energy of −11.9 kcal/mol and RMSD of 0.00 are surrounded by hydrophobic residues. In Fig. 4A, quinoxaline and thiadiazoles ring is bounded by hydrophobic pockets consisting of amino residues such as Gly437, Ile426, Act500, Ile72, Tyr69, Phe351, Glu270, Ile105, Leu166, Ala204, Lys203, Glu419, Ile205, and four hydrogen bonding of Arg4309 (2.92 A°), His44 (2.87 A°), Gly438 (2.87 A°) and Asn423 (3.11 A°). This insilico study revealed that ligand number 5A showed good binding energy toward the $GABA_{AT}$ protein than other co-ligands (Table 8).

The docked models reveal that O-1, O-3, O-2 and N-2 of the quinoxaline and thiadiazoles ring forms hydrogen bonds with amino acids backbone of Arg4309 (2.92 A°), His44 (2.87 A°), Gly438 (2.87 A°) and Asn423 (3.11 A°) respectively. The hydrogen bonding distance for highly active compound 5a is shown in Fig. 4A. The hydrogen bonding distance for remaining compounds is shown in Table 8. The quinoxaline and thiadiazoles ring play a crucial role in producing biological activity by interacting with Arg4309, His44, Gly438 and Asn423, an important active residue for binding affinity of the inhibitor. These interactions underscore the importance of electronegative elements as such oxygen and nitrogen atoms for binding and subsequent inhibitory capacity.

The decrease in descriptors such as DPSA-1 and WT.eneg in particular will increase the binding affinity and atomic electronegativity of these inhibitors. A critical look at these two descriptors inferred that the binding affinity and atomic electronegativity have to be considered in order for the inhibitory activities of quinoxaline and thiadiazoles derivatives to be effective in inhibiting the activities of $GABA_{AT}$ enzyme, an enzyme responsible for epilepsy. This is in agreement with the result of molecular docking in which compounds 5a (Fig. 4A) with the best binding affinity of −11.9 kcal/mol

Table 8
$GABA_{AT}$ active site residues involved in docking interactions with the inhibitors and docking scores.

Ligand (s)	Receptor	Binding Affinity (kcal/mol)	Interaction residues	Hydrogen bonding	Hydrogen bond length (Å)
1b	$GABA_{AT}$	−9.1	Thr353,Phe351,Phe189,Ans352	Arg192	2.77, 2.81
2a	$GABA_{AT}$	−8.0	His206, Gly440, Cys439, Gly438, Glu270, Lys203		
3a	$GABA_{AT}$	−6.9	Cys439, Glu270, Lys203, Arg422, Asn423,Ile426, Gly440, Arg445, Gly438,	Ser427, Arg430	2.93, 3.00 and 3.24
4a	$GABA_{AT}$	−7.6	Ser427, Asn431, Pro23, Tyr348, Lys203, Arg422, Gly438, Ile426, Asn423,	Arg430	2.92
5a	$GABA_{AT}$	−11.9	Gly437, Ile426, Act500, Ile72, Tyr69, Phe351, Glu270, Ile105, Leu166, Ala204, Lys203, Glu419, Ile205,	Arg4309, His44, Gly438, Asn423.	2.920,2.87, 2.87 and 3.11
6b	$GABA_{AT}$	−7.9	His206, Lys203, Gly440, Cys439	Glu270, Asn423, Glu41, Arg430	2.83, 2.81, 3.21, 3.00 and 3.22
7a	$GABA_{AT}$	−9.1	Val22, Ser427, Lys203, Tyr348, His44, Asn423, Pro23,	Arg430, His206, Arg192	2.81, 3.22, and 3.1
8a	$GABA_{AT}$	−7.5	Lys154, Asn345, Glu41, Pro344	Ser153, Glu341, Asn35, Arg343 And Arg343	2.81, 2.99, 3.04,3.00, 9.29, 2.96 and 2.82
9a	$GABA_{AT}$	7.4	Leu392, His206, Pro399, Ser403, Pro226		
10a	$GABA_{AT}$	−6.7	Arg343, Ile72, Tyr69, Lys424, Ser420, Asn423, His44,		
11a	$GABA_{AT}$	−7.5	Glu41, His206, Ile426, Gly438, Cys439, Gly440, Lys203,	Arg430, Asn423, Glu270, Arg422	2.96, 3.13, 2.90, 2.93, 2.85.
12a	$GABA_{AT}$	−7.4	Gly440, Cys439, Gly438, Glu270, Lys203, Arg422, Asn423, Ser427, Arg445.	Arg430	3.17 and 3.0
13b	$GABA_{AT}$	−9.2	Pro23, Ser427, Asn423, Ile423, Arg422, Tyr348, Arg430	His206, His44, Gly438, Val22	3.14, 3.09, 2.97, 2.90
14a	$GABA_{AT}$	−7.1	Arg404, Ser443, Asp415.		
15b	$GABA_{AT}$	−6.5	Ile72, Tyr348, Ile72, Pro23, Lys203, Arg422.		
16a	$GABA_{AT}$	−10.2	Me31, Arg28, Pro23, Tyr348, Act500, Gly437, Tyr69, Ile26, Arg422,	Gly438, His44, Ala42, Val43, Glu41	2.95, 3.02, 3.20, 3.02, 2.78
17a	$GABA_{AT}$	−10.2	Ile26, Tyr438, Tyr69, Me31, Ala40,	Gly438, Ala42 Glu41, Val143 His44, Gly438	3.04, 3.27, 2.80, 2.89, 2.95, 3.04
18a	$GABA_{AT}$	−7.2	Me31, Tyr69, Act500, Ile72, Tyr348		
19a	$GABA_{AT}$	−9.0	Phe351, Ile105, Ile72, Tyr69, Lys424, Ser420, Asn423, His44, Glu270, Act500, Phe351, Ile105.	Tyr348, Ser427	3.18, 2.95
20b	$GABA_{AT}$	−8.7	Ile72, Act500, Glu270, Tyr348, His206, Ser427, Pro23.	Arg430, His44, Tyr69	3.13, 3.20, 3.00
21a	$GABA_{AT}$	−8.3	Tyr69, Act500, Arg192, Tyr348, His44, Ile205, Leu166, Phe161, Lys203.	Glu270	3.05
22a	$GABA_{AT}$	−9.3	Glu270, His260, Tyr348, Asn423, Me31, Tyr69, Act500, Ile105, Phe351, Ile72, Pro23	Arg430, Ser427	2.93, 2.91
23b	$GABA_{AT}$	−9.4	Ile72, Tyr348, Arg430, Met31, His44, Ser427		
24a	$GABA_{AT}$	−9.6	Ala40, Me31, Tyr348, His206, Arg422, Gly437, Ile426, Arg430, His44,	Val43, Glu341, Ala42, Gly438	2.91, 2.83, 3.26, 2.88
25a	$GABA_{AT}$	−9.5	Pro23, His44, Arg422, Ile426, Tyr69, Tyr348, Me31, Arg28,	Glu41, Val43, Ala42, Gly438, His206	2.80, 2.96, 3.21, 3.19, 3.04.
26b	$GABA_{AT}$	−8.0	Asn274, Ser443, Met186, Lys442, Gly271, Lys203, Leu166, Met170, Arg274	Ser202, Asp441, Ala204	2.99, 3.08, 3.08.
27a	$GABA_{AT}$	−8.8	Glu270, Tyr69, Ile72, Tyr348, Phe351, Ile105, His44, Ser427, Act500,	Arg430, Asn423, Gly438	3.02, 3.13, 3.21
28a	$GABA_{AT}$	−6.6	Asp441, Ser202, Lys203, Leu166, Ala204, Met170	Ile205	3.03
29a	$GABA_{AT}$	−6.7	Arg404, Ser443, Asp415, Asn274, Met186, Arg222, Lys44	Gly272, Ser443, Phe220	3.09, 3.26, 2.98,3.10
30b	$GABA_{AT}$	−5.8	Leu392, Gln228, Pro399, Ser403,		
31a	$GABA_{AT}$	−7.4	Glu341, Trp150, Arg343, Asn345, Ser159, Arg156,	Gly157, Ser153	3.26, 2.80 and 2.91
32a	$GABA_{AT}$	−5.8	Ala174, Cys177, Asp179, Phe213, Ser212, Asp214, Gln173,	Ser212, Asn172	3.04, 2.86
33a	$GABA_{AT}$	−7.9			
34b	$GABA_{AT}$	−7.9	Glu270, Tyr348, His206, Ile426, His44, Lys203	Gly438, Tyr69	3.12, 3.31, 3.00
35a	$GABA_{AT}$	−7.3	His44, Ile426, Tyr348, His206, Asn423, Glu419, Ala42, Arg430	Arg422, 3.08	3.14, 3.08
36b	$GABA_{AT}$	−8.3	Tyr69, Act500, Phe351, Ile105, Ile72, Tyr348, Arg430, Met31, Glu41, Val143, His44, Asn423, Cys439, Glu270.		
37a	$GABA_{AT}$	−6.5	Tyr225, Leu392, Gln228, Pro399, Ser403, Pro226, Leu227, Val405, Gln395		

is bounded by hydrogen bond to amino acid residues through the electronegative atoms such as oxygen (O-1, O-3, O-2) and nitrogen (N-2) of the ligand number 5A ring.

Therefore, it can be inferred that the quinoxaline and thiadiazoles derivatives are good anticonvulsant compounds that possessed inhibiting potential against an enzyme that is responsible for epilepsy ($GABA_{AT}$ enzyme).

4. Conclusion

The approach used in this research was successful in finding novel $GABA_{AT}$ inhibitors from the data set developed by computational methods. The robustness and applicability of the QSAR models have been established by internal and external validation techniques. It has been revealed that the dominant structural features responsible for the inhibitory activity of quinoxaline and thiadiazoles derivatives against an enzyme responsible for epilepsy ($GABA_{AT}$) were physiochemical parameters such as minHBint4, ETA_Alpha, DPSA-1, GRAV-5, and WT.eneg. In docking analysis, Compound 5a indicated higher binding affinity with docking score of −11.9 kcal/mol against $GABA_{AT}$ than other co-ligands. From the docking analysis, we realized that the binding scores generated were found to be better than the one proposed by another researcher [39].

The physicochemical descriptors used in QSAR analysis (model 1) in this study were important parameters to consider in improving the potency of these substituted quinoxalines and thiadiazoles derivatives as inhibitors of $GABA_{AT}$. Our QSAR model and molecular docking results corroborate with each other (most especially in the area of binding affinity and atomic electronegativity of the inhibitors) and propose the directions for the design of new inhibitors with better activity toward $GABA_{AT}$ an enzyme responsible for epilepsy.

Conflict of interest

No conflict of interest.

Funding

The authors received no direct funding for this research.

Compliance with ethics requirements

This article does not contain any studies with human or animal subjects.

References

[1] Yemadje LP, Hoinonato D, Quent F, Druet-Cabanac M, Preux PM. Understanding the differences in prevalence of epilepsy in tropical regions. Epilepsia 2011;52:1376–81.
[2] Guerrini R. Epilepsy in children. Seminar at Department of child Neurology and Psychiatry. University of Pisa and IRCCS Foundazionestella Maris; 2006:367;499–524.
[3] Dantas FG, Cariri GA, Filho AR. Knowledge and attitudes towards epilepsy among primary, secondary and tertiary level teachers. Neurology-Psiquiatar 2001;59:712–6.
[4] Kabir M, Iliyasu Z, Abubakar IS, Kabir ZS, FarinYaro AU. Knowledge, attitude and belief about epilepsy among adults in a Northern Nigeria Urban community. Ann Africa Med 2012;4:107–12.
[5] Atshunler LL. Depression, anxiety and temporal lobe epilepsy. Laterality of focus and symptoms. Arch Neurol 1990;4:284–8.
[6] Osolodkin KI, Chupakhin VI, Palyulin VA, Zefirov NS. Molecular modeling of ligand-receptor interaction in GABAc receptor. J Mol Graphics Mod 2009;7:813–21.
[7] Smith AJ, Simpson PB. Methodological approaches for the study of GABAA receptor pharmacology and functional responses. Anal Bioanal Chem 2003;377:843–51.
[8] Karlsson A, Fonnum F, Malthe-Sorenssen D, Storm-Mathisen J. Effect of the convulsive agent 3 mercaptopropionic acid on the levels of GABA, other amino acids and glutamate decarboxylase in different regions of the rat brain. J Biochem Pharmacol 1974;23:3053–61.
[9] Krogsgaard-Larsen P. Gamma aminobutyric acid agonists, antagonists, and uptake inhibitors: design and therapeutic aspects. J Med Chem 1981;24:1377–83.
[10] Storici P, Capitani G, Baise DD, Moser M, John RA, Jansonius JN, et al. Crystal structure of GABA aminotransferase, a target for antiepileptic drug therapy. Biochemistry 1999;38:8628–34.
[11] Xu T, Bajjalieh SM. SV2 modulates the size of the readily releasable pool of secretory vesicles. Nat Cell Biol 2002;3:691–8.
[12] Dichter MA, Brodie MJ. New antiepileptic drugs. English J Med 1996;336:1583–90.
[13] Malawsk BA, Gobaill S. Synthesis, physicochemical and pharmacological properties N-substituted amides of α-piperazine-gamma-hydroxybutyric acid. Phamarzie 1995;50:390.
[14] Yuriev E, Agostino M, Ramsland PA. Challenges and advances in computational docking: in review. J Mol Recognit 2009;24:149–64.
[15] Mura C, McAnany CE. An introduction to biomolecular simulations and docking. Mol Simul 2014;40:732–64.
[16] Tantar AA, Conilleau S, Parent SB, Melab N, Brillet L, Roy S, et al. Docking and biomolecular simulations on computer grids: Status and trends. Curr Comput-Aided Drug Des 2008;4:235–49.
[17] Hansch C, Leo A, Exploring QSAR. Fundamentals and applications in chemistry and biology. Washington, DC: American Chemical Society; 1995.
[18] Kubinyi H. Drug Discovery Today 1997;2:457–67.
[19] Ivanciuc O. 3D QSAR Models. In: Diudea MV, editor. QSPR/QSAR Studies by Molecular Descriptors. Huntington, N.Y.: Nova Science; 2001.
[20] Hansch C, Leo A, Hoekman DE, Exploring QSAR. Fundamentals and application in chemistry and biology. Washington, DC, USA: Am Chem Soc; 1995.
[21] Marone S, Rozas I, Weaver DF. Theoretical structural analyses of tricyclic neuroactive drugs: quantum pharmacologic descriptors for clustering anticonvulsant, antidepressant, and antipsychotic activities. J Mol Struct (Theochem) 1999;467:25–30.
[22] Marder M, Estiu MG, Blanch LB, Viola H, Wasowski C, Medina JH. Molecular modeling and QSAR analysis of the interaction of flavones derivatives with the benzodiazepine site of GABAA receptor complex. Bioorg Med Chem 2001;9:323–35.
[23] Verli H, Albuquerque MG, Bicca de Alencastro R, Barreiro EJ. Local intersection volume: a new 3D descriptor applied to develop a 3D-QSAR pharmacophore model for benzodiazepine receptor ligands. Eur J Med Chem 2002;37:219–29.
[24] Jin AJ, Kohn H, Béguin C, Andurkar SV, Stables JP, Weaver DE. A quantitative structure activity relationship study for Alpha_-substituted acetamido-N-benzylacetamide derivatives – A novel anticonvulsant drug class. Can J Chem 2005;83:37–45.
[25] Kikkeri P. Harish A. Kikkeri N. Mohana N. Lingappa M. Synthesis of indazole substituted-1,3,4-thiadiazoles and their anticonvulsant activity; drug invention today 2013;5:9 2–9.
[26] Kikkeri P. Harish KN. Mohana A, et al. Synthesis of pyrazine substituted 1,3,4-thiadiazole derivatives and their anticonvulsant activity. Hindawi Publishing Corporation Organic Chemistry International; 2013. p. 8.
[27] Mohamed A. Adel G. Ahmed EL. Lingappa M. Synthesis and biological evaluation of some [1,2,4]Triazolo[4,3-a]quinoxaline derivatives as novel anticonvulsant agents. Hindawi Publishing Corporation Organic Chemistry; 2013. p. 7.
[28] Ruba S, Aroo M, Naz G. IOSR J Pharm Biol Sci 2014;9:15–23.
[29] Anonymous. Wavefunction. Inc., Spartan'14, version 1.1.2. Irvine, California, USA; 2013.
[30] Trott O, Olson AJ. AutoDock Vina: improving the speed and accuracy of docking with a new scoring function, efficient optimization, and multithreading. J Comput Chem 2010;31:455–61.
[31] Morris GM, Huey R, Lindstrom W, Sanner MF, Belew RK, Goodsell DS, et al. J Comput Chem 2009;3:2785–91.
[32] Accelrys Software Inc., Discovery Studio Visualizer 4.1, Accelrys Software Inc., San -Diego, CA, USA; 2013.
[33] Yap Chun Wei; Inc., PaDEL-Descriptor,version 2.18; 2011.
[34] Ravinchandran V, Rajak H, Jain A, Sivadasan S, Varghese CP, Kishore-Agrawal R. Validation of QSAR models-strategies and importance. Int J Drug Des Discov 2011;2:511–9.
[35] Myers RH. Classical and modern regression application. 2nd ed. CA: Duxbury Press; 1990.
[36] Stanton DT, Jurs PC. Development and use of charged partial surface area structural descriptors in computer assisted quantitative structure property relationship studies. Anal Chem 1990;62:2323–9.
[37] Stanton DT, Dimitrov S, Grancharov V, Mekenyan OG. Charged partial surface area (CPSA) descriptors QSAR applications. SAR and QSAR Environ Res 2002;13 (2):341–51.
[38] Todeschini R, Gramatica P. New 3D molecular descriptors: the WHIM theory and QSAR applications. Perspect Drug Discovery Des 1998:355–80.
[39] Iftikhar H, Batool S, Deep A, Balasubramanian N, Prabodh CS, Manav M. In silico analysis of the inhibitory activities of GABA derivatives on 4-aminobutyrate transaminase. Arabian J Chem 2013;03:007.